



The Holocene thermal maximum and late-Holocene cooling in the tundra of NE European Russia

J. Sakari Salonen ^{a,*}, Heikki Seppä ^a, Minna Väliranta ^b, Vivienne J. Jones ^c, Angela Self ^c, Maija Heikkilä ^{a,d}, Seija Kultti ^a, Handong Yang ^c

^a Department of Geosciences and Geography, PO Box 64, University of Helsinki, Helsinki 00014, Finland

^b Department of Environmental Sciences, University of Helsinki, Helsinki, Finland

^c Environmental Change Research Centre, Department of Geography, University College London, London, UK

^d Department of Earth and Environmental Sciences, University of Waterloo, Waterloo, Ontario, Canada

ARTICLE INFO

Article history:

Received 3 September 2010

Available online 22 February 2011

Keywords:

Summer temperature

Pollen

Plant macrofossils

Stomata

Transfer function

ABSTRACT

To investigate the Holocene climate and treeline dynamics in the European Russian Arctic, we analysed sediment pollen, conifer stomata, and plant macrofossils from Lake Kharinei, a tundra lake near the treeline in the Pechora area. We present quantitative summer temperature reconstructions from Lake Kharinei and Lake Tumbulovaty, a previously studied lake in the same region, using a pollen–climate transfer function based on a new calibration set from northern European Russia. Our records suggest that the early-Holocene summer temperatures from 11,500 cal yr BP onwards were already slightly higher than at present, followed by a stable Holocene Thermal Maximum (HTM) at 8000–3500 cal yr BP when summer temperatures in the tundra were ca. 3°C above present-day values. A *Picea* forest surrounded Lake Kharinei during the HTM, reaching 150 km north of the present taiga limit. The HTM ended with a temperature drop at 3500–2500 cal yr BP associated with permafrost initiation in the region. Mixed spruce forest began to disappear around Lake Kharinei at ca. 3500 cal yr BP, with the last tree macrofossils recorded at ca. 2500 cal yr BP, suggesting that the present wide tundra zone in the Pechora region formed during the last ca. 3500 yr.

© 2011 University of Washington. Published by Elsevier Inc. All rights reserved.

Introduction

In the coming decades global warming is expected to be strongly expressed in the Arctic region, including the Arctic treeline zone in northern Eurasia where a warming of several degrees is predicted by the end of the 21st century (Christensen et al., 2007; Meehl et al., 2007). The climate warming is expected to cause a significant northward shift of the treeline which is projected to reach the Arctic Ocean coast across most of northern Eurasia (Kaplan et al., 2003; ACIA, 2004; Fischlin et al., 2007; MacDonald et al., 2008; MacDonald, 2010). A major treeline advance could lead to further warming, with possible positive net feedback due to the decreasing albedo of the treeline and the tundra zone (Foley et al., 1994, 2003; Betts, 2000; ACIA, 2004; Chapin et al., 2005; Winton, 2006; Bonan, 2008; Miller et al., 2010a; Swann et al., 2010), making the understanding of Arctic treeline dynamics one of the key tasks in global change research.

The study of past climate changes and associated treeline shifts in the Arctic can be used to analyse the climate-sensitivity of the treeline and to predict its position and species composition under future climate scenarios in different parts of the circumpolar treeline

(e.g., Payette et al., 2002; Seppä et al., 2002; Bigelow et al., 2003; Kaplan et al., 2003; Tinner et al., 2008; MacDonald et al., 2008; MacDonald, 2010). To obtain this goal, a network of sites analysed for palaeoecological proxies is required. In this study we present new data on the Holocene palaeoclimate of the northeastern part of European Russia. This area, located on the Arctic Ocean coast just west of the Ural Mountains, constitutes a major part of the European side of the Eurasian treeline zone, and is characterised by a treeline mostly formed by spruce and a 100–200 km wide tundra zone north of it. The modern treeline and tundra zone between the White Sea and the Ural Mountains might have been mostly ice-free through the last glacial maximum (Svendsen et al., 2004). Early- and mid-Weichselian ice-sheet advances have been suggested as more extensive in this region, reaching further south into the land area of present-day northeast European Russia (Svendsen et al., 2004). Past changes of the treeline in the region have been inferred from radiometric dating of tree megafossils (Khotinskiy, 1984; Kremenetski et al., 1998; MacDonald et al., 2000; see also Binney et al., 2009) and biostratigraphical studies employing pollen and other proxies (Khotinskiy, 1984; Velichko et al., 1997; Serebryanny et al., 1998; Tarasov et al., 1998; Andreev and Klimanov, 2000; Kaakinen and Eronen, 2000; Andreev et al., 2001; Oksanen et al., 2001; Bigelow et al., 2003; Kultti et al., 2003, 2004; Paus et al., 2003; Sarmaja-Korjonen et al., 2003; Väliranta et al., 2003, 2006; Cremer et al., 2004). These and other earlier studies have

* Corresponding author. Fax: +358 9 19150826.

E-mail address: sakari.salonen@helsinki.fi (J.S. Salonen).

established the Holocene expansion of the treeline following the end of the last glaciation. Typically the treeline reached its northernmost position by the mid-Holocene thermal maximum (HTM). Previous studies have also provided general insights into the past climate changes, but in terms of quantitative palaeoclimate estimates the past development of the northern Eurasian treeline zone remains poorly understood.

In order to investigate the Holocene palaeoclimatology and the associated history of the treeline in northeast European Russia more accurately, we produced pollen, stomatal, and plant macrofossil records from a sediment core obtained from Lake Kharinei, located in the tundra, about 75 km north of the modern treeline. In addition, we constructed a new pollen–climate calibration set from Russia and used it to reconstruct quantitatively summer temperature from pollen–stratigraphical data from Lake Kharinei and Lake Tumbulovaty, a previously investigated lake lying just north of the treeline ca. 150 km west of Lake Kharinei. The analysis and results of Lake Kharinei are discussed in detail here. Lake Tumbulovaty has been previously discussed by Kultti et al. (2004) and only the new palaeoclimate reconstruction is presented here. Lake Kharinei is also discussed by Väliaranta et al. (2011), as part of a multi-site study which focuses on late-glacial and early-Holocene vegetation dynamics, and Jones et al. (in press) in a palaeolimnological work which analyses the effects of Holocene treeline shifts on the Lake Kharinei ecosystem. In addition to the quantification of the summer temperature changes, we focus particularly on using plant macrofossil data for identifying the Holocene history of *Picea*, the key treeline species in the region, on determining the location of the *Picea* distribution limit during the HTM between the modern treeline and the Arctic Ocean coast in the north and using the macrofossil evidence for validating the pollen-based temperature reconstruction.

Study area

Lake Kharinei (67°22'N 62°45'E, surface elevation 110 m a.s.l.) is located in the Pechora River basin in the Nenets Autonomous District, northern Russia. The Pechora basin is lined by the northern Ural Mountains in the east and by the Timan Ridge in the west. Lake Kharinei lies in a north-south trending topographic depression. The lake measures ca. 2 km in length and 250 m in width and has a maximum measured water depth of 16 m. The surrounding area is

mostly flat, low-lying (elevation 100–200 m a.s.l.) tundra. The Ural Mountains run about 100 km to the southeast and the shoreline of the Barents and Kara Seas about 200 km to the north of Lake Kharinei (Fig. 1).

Mean annual temperature in the Pechora basin varies between 0°C and –7°C, with the coldest temperatures in the northeast where Lake Kharinei is located. Continentality index (Gorczyński, 1920, 1922) is ca. 35–50, increasing from the Barents Sea coast towards the northern Urals. Mean annual precipitation ranges from ca. 400–450 mm in the northern tundra to ca. 650 mm in the taiga in the south (climate parameters calculated based on the WorldClim 1961–90 climate grids of Hijmans et al. (2005)). The modern arctic treeline, formed by *Picea abies* ssp. *obovata*, is situated about 75 km south of Lake Kharinei (Virtanen et al., 2004). The treeline marks the northern limit of the forest–tundra zone, which constitutes an open-woodland transition zone between the tundra and the northernmost taiga forests. In the Pechora region around Lake Kharinei the forest–tundra zone averages about 100 km in width. However, scattered stands of *Picea* can be found tens of kilometres north of the treeline proper, growing on sheltered sites such as river margins and well-drained upland soils. The northern limit of taiga forest, composed mainly of *Picea abies* ssp. *obovata* and *Betula pubescens* with *Pinus sylvestris* locally present on mire margins and on well-drained soils, lies about 150 km south of Lake Kharinei (Fig. 1; Taskaev et al., 1996; Rekacewicz, 1998). Permafrost in the Lake Kharinei region is predominantly discontinuous (50–90% of ground frozen). Transitions to mainly continuous permafrost (90–95%) and sporadic permafrost (10–50%) occur ca. 25 km to the north and 25 km to the south, respectively (Mazhitova and Oberman, 2003).

Lake Kharinei lies near the Markhida line (Mangerud et al., 1999), a moraine belt which marks the largest extent of Weichselian glaciation in the region between the White Sea and the Urals. Svendsen et al. (1999, 2004) consider this to be the southward expansion of the Kara–Barents Ice Sheet which occurred in the early Weichselian, before 80 ka. A large ice-dammed lake, Lake Komi, formed in front of the early-Weichselian ice sheet, draining across the Timan Ridge towards the Baltic Sea basin (Mangerud et al., 2004). Svendsen et al. (2004) suggest that during the last glacial maximum (LGM) the ice sheet margin remained off the present-day shoreline, some 350 km to the northwest of Lake Kharinei (Fig. 1).

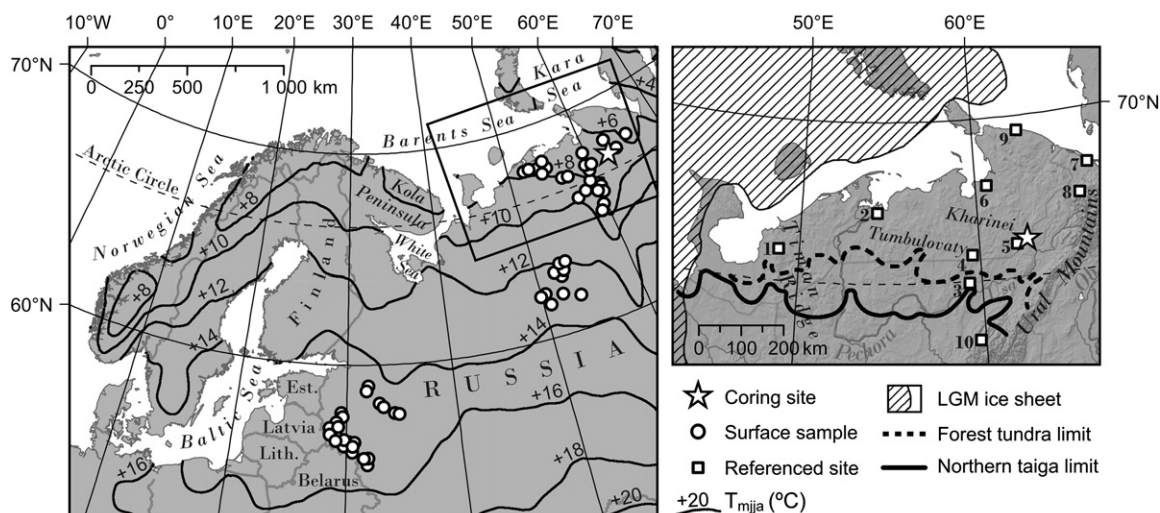


Figure 1. Map of the study area. A rectangle in the larger map shows in the extent of the smaller map. Treeline data is shown based on Rekacewicz (1998) and last glacial maximum (LGM) ice sheet extent on Svendsen et al. (2004). Modern May-to-August mean temperature (T_{mja}) is calculated based on Hijmans et al. (2005) climate grids. Names and references for the numbered sites: 1: Timan Ridge (Paus et al., 2003); 2: Ortino (Kaakinen and Eronen, 2000; Väliaranta et al., 2003); 3: Llet-Ti (Väliaranta et al., 2006); 4: Tumbulovaty (Kultti et al., 2004); 5: Rogovaya (Oksanen et al., 2001); 6: Khaipudurskaya Guba (Velichko et al., 1997; Andreev and Klimanov, 2000); 7: Baidaratskaya Guba (Andreev and Klimanov, 2000); 8: Lyadhej-To (Cremer et al., 2004; Andreev et al., 2005); 9: Cape Shpindler (Andreev et al., 2001); 10: Mezghornoe (Kultti et al., 2003).

Materials and methods

Fieldwork and sampling

Lake Kharinei was cored from the ice in April 2007 using Russian corers with 50- and 100-cm-long chambers. The coring site was 30 m from the shore with a water depth of 780 cm. A 320-cm sediment sequence was retrieved in five overlapping core samples until the bottom of the core (sand) was reached. Core samples were wrapped in plastic. The top section of the sediment was additionally sampled with a Renberg gravity corer. In the laboratory the samples were split at 1 cm intervals and stored in plastic bags at +4°C. Surface sediment samples for the pollen–climate calibration model were collected during several field seasons in 1998–2007. The samples were collected from the centre of medium-sized lakes using a surface sediment sampler.

Dating

Fourteen bulk sediment samples were radiocarbon-dated by in the NERC Radiocarbon Facility (Environment) and SUERC AMS Laboratory. Samples were acid digested (2 M HCl, 80°C, 8 hours), washed, dried and homogenised. The total carbon was recovered as CO₂ by heating with CuO and the gas converted to graphite by Fe/Zn reduction. These dates were supplemented by seven terrestrial plant macrofossil dates. Macrofossil material in the base of the core was insufficient for radiocarbon dating. These samples were dated in the Poznan radiocarbon laboratory. All the dates were calibrated using IntCal09 (Reimer et al., 2009) in OxCal 4.1 (Bronk Ramsey, 1995, 2009). Age–depth models were produced in the R statistical software (R Development Core Team, 2008) using the function of Heegaard et al. (2005). The top 3 cm of the core was also dated with ²¹⁰Pb. Dried sediment samples were analysed for ²¹⁰Pb, ²²⁶Ra, ¹³⁷Cs and ²⁴¹Am by direct gamma assay in the Bloomsbury Environmental Isotope Facility (BEIF) at University College London. ²¹⁰Pb chronologies were calculated using the CRS dating model (Appleby and Oldfield, 1978) and corrected by the ¹³⁷Cs/²¹⁰Pb records.

Bio- and lithostratigraphical analyses

Pollen samples from the Lake Kharinei sequence and the surface sites were prepared using KOH, HF and acetolysis treatments (Fægri and Iversen, 1989). They were prepared at 2 cm intervals in the top 80 cm and at 4 cm intervals from the rest of the core (100 samples) and at least 350 pollen and spores were counted, with most counts reaching 500. From the surface samples a minimum of 500 terrestrial pollen and spores were counted. *Lycopodium* tablets (Stockmarr, 1971) were added to samples for calculation of pollen accumulation rates (PAR) based on the sedimentation rates indicated by the age–depth model. Percentage values for pollen and spores of terrestrial plants, charcoal fragments and *Pediastrum* were calculated from the sum of terrestrial pollen and spores. Aquatic pollen was included in the sum used for aquatic pollen percentages. Pollen nomenclature follows Moore et al. (1991). Conifer stomata were identified from pollen slides according to Sweeney (2004).

Plant macrofossil analysis on Lake Kharinei was carried out at 4 cm resolution. The sediment volume was determined by displacement of water in a measuring cylinder. The volume varied between 2 and 15 cm³ but was typically 5 or 10 cm³. The sediment was soaked in Na₄P₂O₇ × H₂O (sodium pyrophosphate) solution in order to break the mineral clusters. The sediment was sieved through a 124 µm mesh and the residue was systematically examined using a stereo-microscope and a high magnification light microscope.

Lithology was first analysed based on visual observation in the field. Loss-on-ignition (LOI) measurements were done in the laboratory at two-centimetre intervals.

Pollen–climate transfer function

A pollen–climate transfer function (cf. Seppä and Birks, 2001; Birks and Seppä, 2004; Seppä et al., 2004) was constructed for northern European Russia. The transfer function is based on a calibration model which uses surface sample pollen assemblage data from 58 sites across the northern parts of European Russia. The pollen–climate relationship is modelled based on the surface site pollen assemblages and the modern climate parameter values at the sites. Our surface sample sites for the pollen–climate calibration set form a discontinuous, 2200-km transect from southwest to northeast across European Russia, from the Latvian and Belarussian borders to the northern Ural Mountains (Fig. 1). The sites are concentrated in three different areas representing different vegetation types of European Russia. The southwesternmost sites are located in the mixed forest zone in Novgorod, Pskov, Tver, and Smolensk provinces. A central group is found in the taiga zone in the southern part of Komi Republic. The northeastern sites lie around the treeline zone and in the tundra in the Nenets Autonomous District and the northern part of Komi Republic.

The transfer function was calculated using weighted averaging–partial least squares (WA-PLS) regression (ter Braak and Juggins, 1993; Birks, 1998) in the C2 computer programme (Juggins, 2007). The calibration set for the transfer function includes surface sediment pollen assemblage data and modern temperature values for the 58 surface sites, all medium-sized lakes selected with consistent criteria (Seppä et al., 2004). The calibration set species data consist of percentage values for 72 land plant pollen and spore types found in the surface samples, square-root transformed to reduce noise in the data (Prentice, 1980). All samples and taxa were included in the calibration set. A modern summer temperature estimate (May-to-August mean, T_{mija}) for each calibration set site was calculated, using the ArcInfo GIS software, based on the WorldClim 1961–90 climate grids (Hijmans et al., 2005). T_{mija} was chosen as climate parameter as it roughly represents the temperature conditions during the growing season, including late spring, generally the most important single climate factor influencing the distribution, reproduction and growth of the plants in the arctic region (Hinzman et al., 2005; Euskirchen et al., 2009). Modern T_{mija} values at the calibration set sites range from +5.9°C near the Polar Urals to +15.6°C in the western Russian sites (Fig. 1).

Transfer functions were developed based on the pollen and modern climate data using one-, two-, and three-component WA-PLS regression. The performance of all three transfer functions was evaluated by leave-one-out cross validation (Birks et al., 1990), i.e., by predicting the modern temperature of each surface site based on all surface sites except the one in question, and by then comparing the predicted modern temperatures at all sites to observed temperatures. Performance statistics for the three transfer functions are presented in Table 1. The two-component transfer function was selected due to lowest root mean square error of prediction (RMSEP) and highest r^2 (coefficient of determination) between predicted and observed values. RMSEP for the selected transfer function is 1.121°C or 11.6% of observed temperature range, with an r^2 of 0.882 between predicted and observed temperatures. The relationship between predicted and observed temperatures is shown in Figure 2. Overall, the performance is most robust at warmer temperatures. At taiga sites (observed

Table 1

Performance statistics for 1-, 2-, and 3-component pollen–climate WA-PLS regression models using leave-one-out cross validation. Reported statistics are root mean square error of prediction (RMSEP), coefficient of determination (r^2), and maximum bias.

WA-PLS components	RMSEP	r^2	Maximum bias
1	1.353°C	0.828	2.428°C
2	1.121°C	0.882	1.629°C
3	1.206°C	0.863	1.536°C

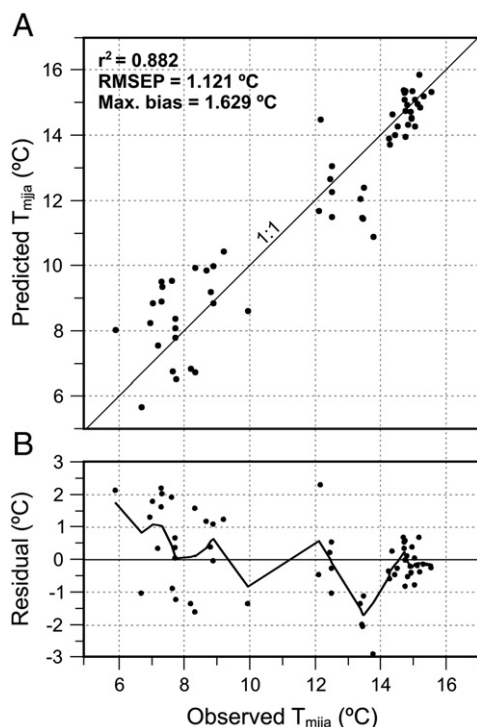


Figure 2. Transfer function performance based on the 2-component WA-PLS model. (A) Predicted vs. observed temperature. (B) Residuals of predicted temperature vs. observed temperature. A LOESS smoother (span 0.25, one robustifying iteration) is fitted through the data.

temperature 12–14°C) the majority of predicted temperatures are below the observed, while at tundra and forest–tundra sites (observed temperature <10°C) there is a tendency to overestimate temperatures.

A T_{mja} reconstruction was prepared in the C2 software based on the Lake Kharinei fossil pollen sequence using the two-component WA-PLS transfer function. The Lake Kharinei fossil data includes 59 land pollen and spore taxa of which 47 were also found in the calibration set. Sample-specific errors of reconstructed palaeotemperature values were estimated by Monte Carlo simulation based on a 100-cycle bootstrapping procedure (Birks, 2003). Ninety-five percent reconstruction errors are mostly between $\pm 1.2^\circ\text{C}$ and $\pm 1.5^\circ\text{C}$.

Results

Chronology

In our material (Table 2, Fig. 3), there is a general tendency for the bulk sediment ^{14}C dates to be older than macrofossil ^{14}C dates from nearby levels. While at some depths (e.g. 100 and 280–290 cm) there are similar bulk and macro dates, through most of the cores the bulk dates are ca. 1500–2000 yr older than adjacent macro dates. Pollen-stratigraphical comparisons to other radiocarbon-dated pollen diagrams suggest that the bulk dates at the base of the core showing ages of 12,000–12,500 cal yr BP are too old, as the pollen assemblages from this depth do not resemble the late-glacial assemblages, most notably lacking the high *Artemisia* values which characterise the late-glacial deposits in the Pechora basin (Paus et al., 2003; Välranta et al., 2006) and elsewhere in northern Russia (Snyder et al., 2000; Andreev et al., 2002; Wohlfarth et al., 2002; Velichko et al., 2002). Our findings are similar to other studies in the Pechora area which have shown that bulk sediment ^{14}C dates may be up to ca. 1000 yr older than dates based on terrestrial plant remains from the same subsample (Kultti et al., 2003; Paus et al., 2003; Välranta et al., 2006).

Due to the more consistent nature of the dates from macrofossils, supported by the pollen-stratigraphical features, an age–depth model was developed based solely on the macrofossil dates. One macrofossil date at 63–64 cm depth was regarded as clearly too old, as it gives an age ca. 2000 yr greater than the macrofossil date from 99 to 100 cm and produces a distinct reversal in the age–depth relationship, and was left out of the model. The model was thus constructed using the six accepted macrofossil dates and additionally six ^{210}Pb dates from the top 3 cm. The ^{210}Pb chronology (Table 3) of the uppermost 3 cm suggests a modern age for the top of the sediment with sediment accumulation rates of between 0.01 and 0.05 cm yr^{−1} for about the last 150 yr. The two deepest macrofossil dates at 289–290 and 297–298 cm depth show a slight reversal of the age–depth relationship. However, as it was difficult to validate the accuracy of these dates, we have included both in the model, letting this uncertainty to be reflected in the error margins of the model. A cubic smooth spline age–depth model (Fig. 3) was fitted into the dates using the R function of Heegaard et al. (2005). The weight assigned to each date was the reciprocal of the calibrated uncertainty, thus giving greater weights to ^{210}Pb than ^{14}C dates. The k parameter was reduced to 9 to increase the rigidity of the spline. The mu-variance model was chosen over the constant-variance model due to significantly smaller residuals of

Table 2

Radiocarbon dating results and corresponding calibrated ages. The dated material is bulk sediment (B) or terrestrial macrofossil (M).

Lab code	Depth (cm)	Material	^{14}C age (^{14}C yr BP $\pm 1\sigma$)	Calibrated age (cal yr BP, 95% probability)
SUERC-21513	20–21	B	2663 \pm 37	2742–2848
SUERC-21516	30–31	B	2256 \pm 37	2155–2345
SUERC-17505	40–41	B	2411 \pm 37	2346–2699
Poz-34966	63–64	M	5080 \pm 40	5736–5915
SUERC-21517	72–73	B	4640 \pm 38	5301–5566
Poz-34208	99–100	M	3590 \pm 40	3728–4066
SUERC-21518	100–101	B	3571 \pm 40	3723–3979
SUERC-17506	128–129	B	5555 \pm 38	6290–6406
SUERC-21519	152–153	B	6878 \pm 39	7620–7794
SUERC-21520	172–173	B	7039 \pm 39	7791–7954
Poz-34967	179–180	M	5460 \pm 40	6185–6317
SUERC-17509	200–201	B	7304 \pm 37	8023–8180
Poz-34209	223–224	M	6250 \pm 40	7020–7265
SUERC-21521	228–229	B	8661 \pm 44	9536–9733
Poz-34968	239–240	M	6780 \pm 50	7523–7700
SUERC-21522	254–255	B	10,212 \pm 45	11,755–12,086
SUERC-17510	284–285	B	9738 \pm 43	10,906–11,242
Poz-34210	289–290	M	9440 \pm 50	10,520–11,063
Poz-34969	297–298	M	9200 \pm 50	10,245–10,500
SUERC-21523	300–301	B	10,213 \pm 45	11,756–12,087
SUERC-21526	314–315	B	10,610 \pm 44	12,427–12,664

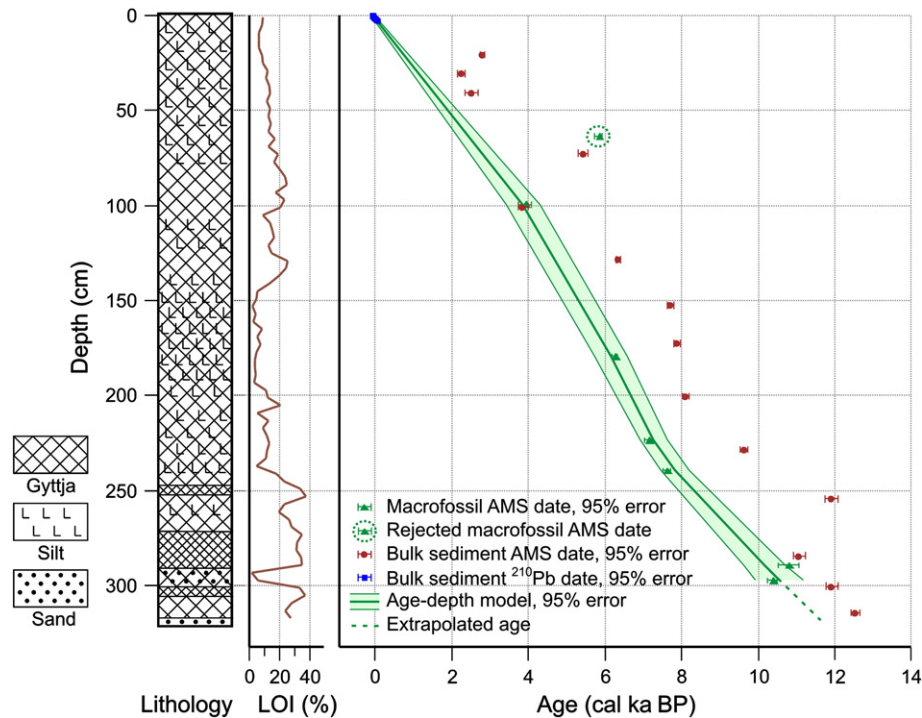


Figure 3. Lake Kharinei lithology, loss-on-ignition (LOI) and an age-depth model constructed based on calibrated terrestrial plant macrofossil ^{14}C ages and ^{210}Pb dating of the top sediment. A cubic smooth spline age-depth model (Heegaard et al., 2005) is fitted into the dates. Age of the bottom section is calculated based on linear extrapolation. Bulk sediment ^{14}C dates and one rejected macrofossil ^{14}C date are also shown.

modelled vs. radiometric ages. Linear extrapolation was used for ages below the last macrofossil date giving an age for the base of the core of ca. 11,500 cal yr BP. As mentioned before, this agrees with the pollen-stratigraphical features of the basal samples. The errors on the model are rather large, the 95% uncertainty interval being about ± 400 yr for most of the core with higher errors at base of the core and smaller errors towards the top section constrained by ^{210}Pb . For the Holocene sediment accumulation rates are fairly linear at ca. 0.03 cm yr^{-1} which compares well with that obtained for the recent sediments by ^{210}Pb .

Bio- and lithostratigraphy

The Lake Kharinei sediment (Fig. 3) is largely homogenous, clayey silt-gyttja with little identifiable layering from the top to 250 cm depth, and with LOI values generally between 7 and 25%, with the exception of a gyttja-silt section at 140–190 cm (LOI 3–5%). Below 250 cm the sediment is mostly gyttja (LOI 20–35%) apart from of a sandy section at 290–300 cm. Coring was stopped at another, impenetrable sandy layer at 320 cm.

The Lake Kharinei pollen stratigraphy that forms the basis for palaeoclimate reconstruction is presented in Figure 4 along with macrofossil records of conifers, *Betula*, and *Alnus*, as well as conifer

stomata. Pollen curves of non-arboreal taxa are high through the early Holocene, with Cyperaceae and Gramineae at around 10% and *Salix* at around 5%. *Equisetum* values are 10–15% during the early Holocene, consistent with other early-Holocene pollen records from the region (Kultti et al., 2003). In terms of arboreal pollen *Picea* and *Pinus* are present in small amounts during this period. *Betula* is consistently abundant (40–60%) through the whole sequence. No attempt was made to distinguish between the pollen of tree-type *Betula* and that of *Betula nana*. In the macrofossils, however, tree *Betula* was counted separately from *B. nana*. Tree *Betula* is dominant during the early Holocene, while *B. nana* is present in smaller quantities. A significant change occurs in the pollen assemblage towards the mid Holocene. The pollen curve of *Picea* rises starting at around 8000 cal yr BP, reaching highest values of 20–30% between ca. 5000–3500 cal yr BP. *Picea* needles and tree *Betula* macrofossils are abundant between 8000 and 2500 cal yr BP and *Picea* stomata are also found between 6000 and 2500 cal yr BP. The pollen curve of *Alnus* shows a mid-Holocene rise in conjunction with that of *Picea*, reaching values around 5%. A distinct reversal in the trends of both pollen and macrofossils occurs around 3500–2500 cal yr BP. The pollen curve of *Picea* falls sharply around this time while curves of non-arboreal taxa, especially Cyperaceae and Gramineae rise. During the same period, total PAR falls from the mid-Holocene values of ca. 1500–3000 to ca. 1000–1500 grains $\text{cm}^{-2} \text{ yr}^{-1}$, by 2500 cal yr BP. No *Picea* stomata or needles are found after ca. 2500 cal yr BP. There are fewer tree *Betula* macrofossils after around 3500 cal yr BP and these virtually disappear at 2500 cal yr BP, while *B. nana* macrofossils become more abundant. The pollen curve of *Pinus* rises after 3500 cal yr BP, which is likely to reflect an increasing proportion of long-range transported pollen as the local pollen production diminished.

Palaeoclimate reconstruction

The Lake Kharinei T_{mija} reconstruction is presented in Figure 5A. T_{mija} values during the early Holocene are somewhat above those reconstructed for the late Holocene, including the modern values.

Table 3
 ^{210}Pb chronology for Lake Kharinei.

Depth cm	Age yr $\pm 2\sigma$	Date AD	Sedimentation rate cm yr $^{-1}$
0	0	2007	
0.25	4 \pm 2	2003	0.05
0.75	17 \pm 3	1990	0.026
1.25	44 \pm 6	1963	0.023
1.75	61 \pm 10	1946	0.025
2.25	83 \pm 18	1924	0.014
2.75	133 \pm 28	1874	0.01

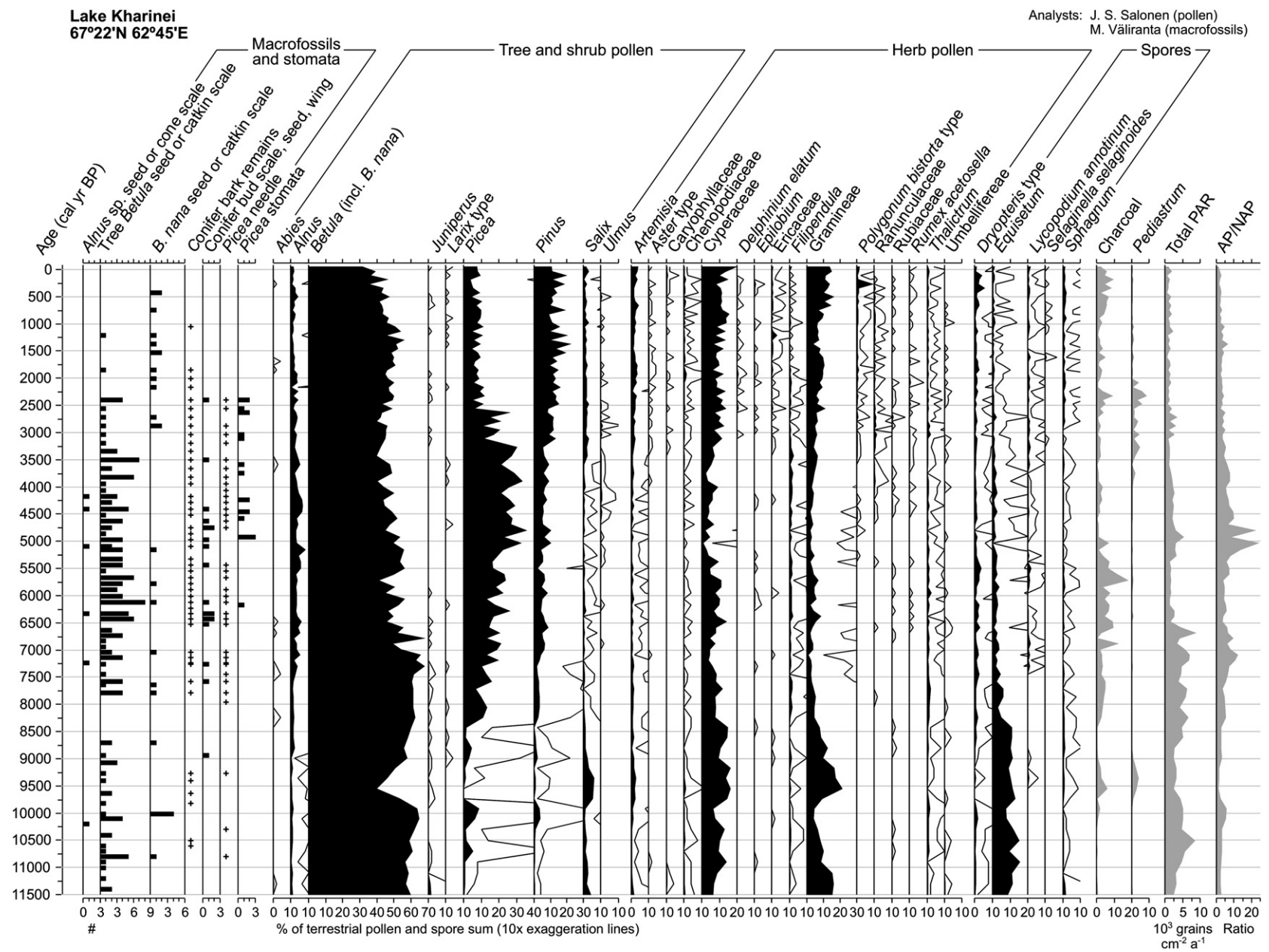


Figure 4. Biostratigraphy of Lake Kharinei. Pollen and spore abundances are shown with black silhouette curves. Macrofossils counted in numbers (such as seeds) and conifer stomata are indicated by bars whereas relative abundance of vegetative remains is indicated by a plus sign. Most abundantly occurring taxa are shown. AP/NAP is calculated as the ratio of the tree and shrub sum and the herb sum.

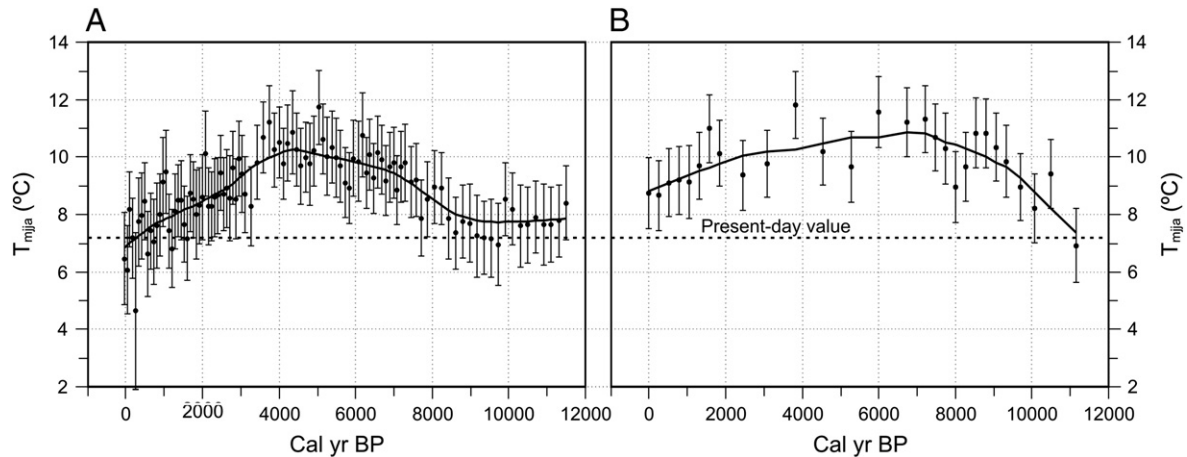


Figure 5. Lake Kharinei (A) and Lake Tumbulovaty (B) T_{mjia} reconstructions. LOESS smoothers (spans 0.25 for Kharinei and 0.45 for Tumbulovaty, one robustifying iteration) are fitted through data. Error bars indicate 95% reconstruction errors estimated with Monte Carlo simulation based on a 100-cycle bootstrapping procedure. Dashed horizontal lines show the modern temperature at Kharinei and Tumbulovaty, calculated based on Hijmans et al. (2005) climate data.

Between 9000 and 6000 cal yr BP T_{mjia} rises gradually, reaching its highest Holocene value of ca. 10°C around 6000–3500 cal yr BP, and remaining so until 3500 cal yr BP. After 3500 cal yr BP T_{mjia} starts to fall, with the most prominent drop at ca. 3500–2500 cal yr BP. A steady decline then continues until present, T_{mjia} falling down to the modern observed value of ca. 7°C, and below the early-Holocene values. At ca. 300 cal yr BP, an outlier of reconstructed T_{mjia} of 4.6°C is due to a sudden, anomalous peak in *Polygonum bistorta* type pollen. This type is sparsely represented in the calibration set with the only specimens found in two of the northeasternmost tundra sites, leading to a cold reconstructed temperature value.

To test the repeatability of the results across the region, a temperature reconstruction for the Holocene is also presented for Lake Tumbulovaty (Fig. 5B) based on the pollen data of Kultti et al. (2004). Lake Tumbulovaty is located ca. 150 km west of Lake Kharinei (Fig. 1). Modern climate grids by Hijmans et al. (2005) indicate a 7.2°C T_{mjia} for both locations. However, it is probable that modern T_{mjia} is higher at Tumbulovaty than at Kharinei, since Tumbulovaty is located at the treeline whereas Kharinei lies ca. 75 km into the tundra. The modern temperature surfaces modelled by Hijmans et al. (2005) are based on just a handful of observation points in and around the Pechora basin, often located several hundred kilometres apart. While the lower resolution of the Tumbulovaty data precludes the assessment of fine palaeoclimate features or exact timing of temperature shifts, the Tumbulovaty T_{mjia} curve supports the major features of the Kharinei reconstruction, indicating also warmest Holocene values for the mid Holocene, between ca. 8000–4000 cal yr BP. Reconstructed Mid-Holocene T_{mjia} values of 10.5–11°C are slightly higher than at Kharinei, in agreement with the location of Tumbulovaty closer to modern-day treeline. The Holocene temperature range is ca. 3°C in both reconstructions.

Discussion

Holocene treeline dynamics

Tree *Betula* macrofossils and *Picea* needles found in the bottom section of Lake Kharinei sediment indicate that these trees were growing in the vicinity of Lake Kharinei around 11,500–10,500 cal yr BP, probably as scattered individuals. The presence of these trees around Lake Kharinei by the start of the early Holocene, and the subsequent gradual increase of tree density reflect the general pattern of forest expansion in the area described by Välranta et al. (2011) who propose that the treeline and tundra zone of the Pechora basin was already patchily vegetated in the late-glacial time by scattered

Picea and tree *Betula* populations and these acted as nuclei for development of more extensive forests during the early Holocene. Based on an assembled body of tree macrofossil datings, Binney et al. (2009) suggest the widely distributed occurrence of *Picea* across Eurasia before and during the LGM. The early postglacial expansion of tree *Betula* beyond its modern limit also suggests either very fast dispersal or local refugia (Binney et al., 2009). The presence of *Picea* and tree *Betula* in the early Holocene, around 11,500–10,500 cal yr BP in the northeastern part of European Russia, at Lake Kharinei, and earlier in the late-glacial time elsewhere in the Pechora basin (Välranta et al., 2006), lends support to the view of scattered, local refugia across northern Eurasia.

The low-frequency occurrence of tree macrofossils suggests that the forest–tundra transition zone had expanded up to Lake Kharinei in the early Holocene. The greater abundance of macrofossils and stomata of *Picea* in the Kharinei record in the mid Holocene (Fig. 4) reflects further advance of the treeline, with a spruce forest mixed with tree birch present in the catchment of the lake, with maximum forest density ca. 6000–3500 cal yr BP. Compared to the present-day situation (Fig. 1), this suggests a minimum 150-km northward expansion of the northern taiga limit during the mid Holocene. Tree macrofossils and *Picea* stomata decrease after 3500 cal yr BP, and then suddenly disappear from the Kharinei record at ca. 2500 cal yr BP (Fig. 4), indicating rapid deforestation. This is associated with subsequent rises of Gramineae, Cyperaceae, and Ericaceae, reflecting the development of the modern tundra in the past ca. 3500 yr, during the southward retreat of the *Picea* range limit.

Despite the new results reported here and in some earlier papers, the assessment of the treeline dynamics and the timing of the major shifts in the Eurasian tundra is hampered by the scarcity of stratigraphic studies with robust dating control and a sufficient time resolution. Lake Kharinei, ca. 75 km north of the modern treeline provides one point of minimum expansion in the Pechora basin, but the northern maximum limit of the *Picea* treeline during the Holocene remains poorly constrained. More stratigraphic studies are needed from further north in the modern tundra, preferably combining pollen analysis with macrofossil and stoma analysis to reliably distinguish between the presence of isolated trees and extensive forest.

Holocene palaeoclimate

Validation of the temperature inferences based on pollen and other fossil proxies is one of the major issues in quantitative palaeoclimatology. When working beyond the timescales of

instrumental observations, a key method is to compare the reconstruction to another, independent climate proxy (Birks, 2003). Plant macrofossils provide one way to validate a pollen-based temperature reconstruction (Birks and Birks, 2003). In the case of Lake Kharinei, the reconstructed T_{mija} during the warm mid-Holocene is 9–10°C, which is similar to the modern T_{mija} value of ca. 9°C at the northern limit of the taiga forest (Fig. 1). Thus the inferred presence of mixed spruce forest around Lake Kharinei based on macrofossils supports the reconstructed T_{mija} value during mid-Holocene (Fig. 6). In the early Holocene ca. 11,500–8000 cal yr BP tree macrofossils are also present in smaller numbers, while they are largely absent in the late Holocene after 2500 cal yr BP, lending credence to the reconstructed early-Holocene pollen-based temperatures which are higher than late-Holocene and modern-day temperatures. The Lake Kharinei macrofossil record therefore supports the major features of the pollen-based reconstruction. Plant macrofossils are not, however, a completely independent proxy from pollen, although they are not used in the transfer function they are also produced by plants. If the distribution ranges of the plant taxa in the past have been in disequilibrium with climate due to factors such as dispersal barriers, soil factors, interspecific competition or slow migration and population growth capacity in relation to faster climate changes (Birks, 1986; Davis, 1986; Ritchie, 1986; Huntley, 1993), both pollen and macrofossils can give a misleading picture of past climates.

The pollen-based T_{mija} reconstructions from Lake Kharinei and Lake Tumbulovaty, combined with the Lake Kharinei tree macrofossil record, suggest a timing of the HTM in the region at around 8000–3500 cal yr BP (Fig. 6). This is markedly similar to the reconstructions from the northern European treeline region. In particular, the quantitative palaeoclimate reconstructions from the Kola Peninsula about 1200 km west of our study region show a clear simultaneous HTM (Jones et al., 2004; Seppä et al., 2008). Likewise in Fennoscandia, Seppä et al. (2009) report similar HTM timing in the mid-Holocene at 8000–4800 cal yr BP from a meta-analysis of 35 pollen-based temperature reconstructions. Based on biostratigraphical studies, comparable HTM timing during the mid-Holocene has been reported around the Pechora basin (Andreev and Klimanov, 2000; Kaakinen and Eronen, 2000) and also in northwest Siberia (Andreev et al., 2002).

The uniform trend of the timing of the HTM from northern Fennoscandia to the Ural mountains is in good agreement with modelling results of Renssen et al. (2009), who use a coupled global ocean–atmosphere–vegetation model to investigate the timing of the HTM in the northern hemisphere. Their results show the HTM peak in our study area at 7–6 cal kyr BP (Fig. 6). Their simulations of northern-hemisphere HTM timing include successive model runs with and without the Laurentide Ice Sheet and its meltwater, albedo and topographic effects. The model suggests that meltwater influx from the remnants of the Laurentide Ice Sheet had an overriding role in delaying HTM relative to the early-Holocene peak in orbital forcing (Fig. 6). The fit between modelled and reconstructed atmospheric temperature suggest a role of North Atlantic circulation in driving climate change in northeast European Russia. The match between our data and that of Renssen et al. (2009) thus implies that the melting Laurentine Ice Sheet has the potential to significantly influence, through thermohaline circulation changes, the summer temperature dynamics 5000–6000 km away on the opposite side of the northern hemisphere.

Some studies in northeast European Russia have indicated an earlier start for HTM, from ca. 11,000 cal yr BP onwards. This is especially the case with some sites located towards the eastern end of the region (sites 8–10 in Fig. 1), in the coastal areas and the Arctic Ocean islands (Serebryanny et al., 1998; Andreev and Klimanov, 2000; Andreev et al., 2001) and in the northern Ural Mountains (Kultti et al., 2003; Cremer et al., 2004; Andreev et al., 2005). Based on pollen- and chironomid-based quantitative reconstructions from the polar Urals, Andreev et al. (2005) suggest highest Holocene mean July temperatures at 10,500–8800 cal yr BP. There are several factors which may contribute to the discrepancies in reconstructed HTM timing. First, there may be a real gradient in HTM timing, possibly connected to LIS meltwater forcing delaying the HTM in more western regions. Second, one or more of the reconstructions may be wrong due to biases in the used temperature inference method. Third, the proxies yielding a mid-Holocene HTM may show a delayed response to summer temperature. Fourth, the complex treeline history of northeast European Russia may account for some of the discrepancies, especially in studies based on pollen and plant macrofossils. Some of the northernmost sites up to the

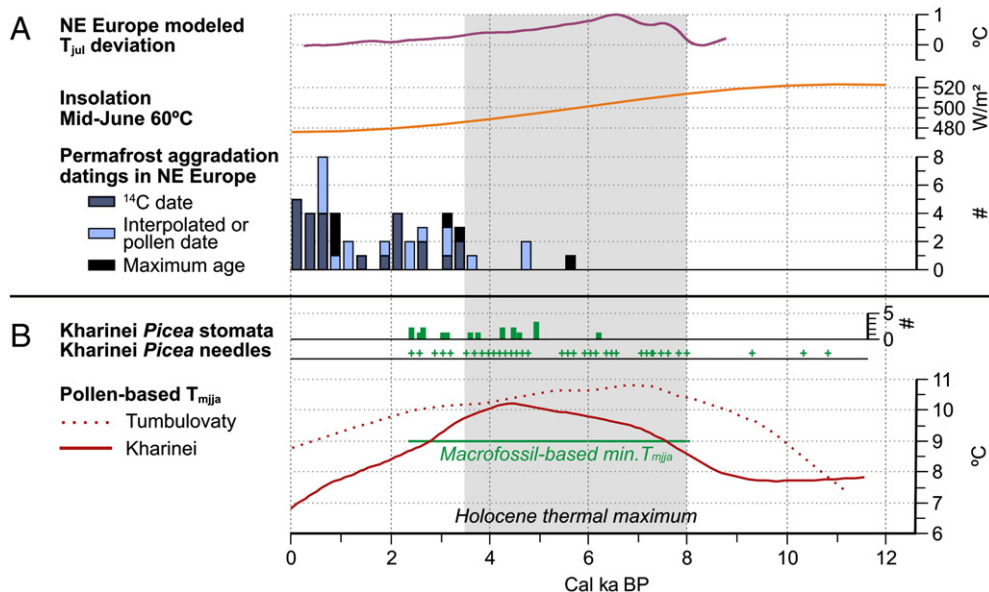


Figure 6. A synthesis of the results and comparison with other data from NE Europe. (A) Supporting data from other studies, listed from top to bottom: Model simulation of NE European climate development during the Holocene (Renssen et al., 2009); Mid-June insolation at 60°N (Berger and Loutre, 1991); Permafrost aggradation datings from northeast Europe. Most data is from the Pechora area and the remainder from northern Fennoscandia (Oksanen, 2005). (B) Lake Kharinei and Lake Tumbulovaty LOESS-smoothed (spans 0.25 for Kharinei and 0.45 for Tumbulovaty, one robustifying iteration) T_{mija} reconstructions and Lake Kharinei *Picea* macrofossil and stomata records. A horizontal line marks the 9°C modern limit of taiga forest, suggested by the macrofossil record to be present in the mid Holocene. The grey band indicates the HTM timing in Northeast European Russia based on the temperature curves and tree macrofossils.

Kara Sea coast show high early-Holocene values of tree *Betula* pollen (sites 1, 8 and 9 in Fig. 1; Andreev et al., 2001, 2005; Paus et al., 2003; Cremer et al., 2004), while these sites are not reached by the mid-Holocene expansion of *Picea*-dominated woodland which is well documented further south in this and other studies (sites 2–6 in Fig. 1; Andreev and Klimanov, 2000; Kaakinen and Eronen, 2000; Oksanen et al., 2001; Välranta et al., 2003, 2006; Kultti et al., 2004). If only the early-Holocene *Betula* expansion is recorded at a site, it may show an earlier reconstructed HTM than a site further south, where the mid-Holocene expansion of *Picea* forest is the dominant change in the fossil assemblage. Thus it is possible that the same treeline history may result in differing palaeoclimate reconstructions depending on the location of the studied site. Due to the scarcity of data currently available, it is not possible to confidently assess the relative roles of the four factors listed above, and spatial patterns of Holocene palaeoclimate in the Northern Eurasian treeline region remain poorly resolved. In future studies, there is a clear need for new palaeoclimatological data from Northern Russia. Additionally, the robustness of the quantitative methodology should be tested, including the evaluation and comparison of the used climate proxies and reconstruction methods.

Another major feature in our reconstruction is the distinct summertime cooling and a southward shift of the treeline in northeast European Russia ca. 3500–2500 cal yr BP. Temperatures in the Lake Kharinei reconstruction fall sharply during that period, together with the retreat of the treeline. Data from other sites in the region suggests that this was a part of a general shift of regional climate and withdrawal of the treeline. The deforestation of the Kharinei site at around 3000 cal yr BP coincides with the disappearance of *Picea* macrofossils at the nearby Tumbulovaty (Kultti et al., 2004) and Rogovaya (Oksanen et al., 2001) sites. In the Pechora delta area, 300 km to the west, disappearance of forests has been dated to ca. 3200 cal yr BP (Välranta et al., 2003). No tree macro- or megafossil finds are reported after 4000 cal yr BP in the present-day tundra of the Pechora basin, in the surveys by Kremenetski et al. (1998) and MacDonald et al. (2000). Falling summer temperatures and treeline withdrawal of the Pechora area in the past 3500 yr constitutes a part of a general trend of late-Holocene cooling and treeline retreat throughout arctic Eurasia (Wanner et al., 2008; Binney et al., 2009; Kaufman et al., 2009; Miller et al., 2010b). In the Pechora basin the late-Holocene cooling coincides with permafrost aggradation, dated to ca. 3200–3000 cal yr BP (Oksanen et al., 2001; Välranta et al., 2003), indicating that the permafrost aggradation in the Pechora region was a part of a broader trend in northern Europe (Fig. 6), with aggradation generally starting in northern Russia ca. 3000 cal yr BP and in Fennoscandia ca. 2500 cal yr BP (Oksanen, 2005).

The declining summer insolation has been clearly shown to be the main driver of the Holocene summer temperature trend (Ganopolski et al., 1998; Wanner et al., 2008; Renssen et al., 2009), particularly after the melting of the Laurentide ice sheet at about 7000 cal yr BP (Renssen et al., 2009). However, our palaeoclimate reconstructions show a deviation between the progression of late-Holocene summertime cooling and the trend in orbital forcing (Fig. 6; Berger and Loutre, 1991). While mid-June insolation diminishes gradually through the Holocene, T_{mija} in the Pechora region stays relatively unchanged, ca. 3°C above present-day values, through the mid Holocene until ca. 3500 cal yr BP, when the fall of T_{mija} towards its present-day values occurs in conjunction with withdrawal of treeline and initiation of permafrost. This suggests that there is a non-linear response of the summer air temperature to decreasing summer insolation, with climate staying relatively unchanged until a threshold condition is reached, triggering a rapid cooling. Similar abrupt mid- to late-Holocene vegetation and climate responses to decreasing insolation have been documented for example in the Sahara desert (deMenocal et al., 2000) and in southern Scandinavia (Seppä et al., 2005; see also Steig, 1999). The rapid treeline withdrawal which seems to have occurred in the Pechora basin around this time and its albedo effects, as well as

permafrost aggradation are possible positive feedback processes involved in the rapid temperature fall. In view of 21st-century climate projections for Arctic Eurasia (Meehl et al., 2007), the great treeline shifts and changes in permafrost conditions involved with our reconstructed Holocene temperature shifts of ca. 3°C suggest the potential for significant environmental changes in the northern Eurasian treeline zone due to increased greenhouse gas forcing.

Conclusions

- In the early Holocene T_{mija} remained steady until ca. 9000 cal yr BP, followed by a gradual rise, culminating in a clear and stable HTM at 8000–3500 cal yr BP. During this time a mixed spruce forest surrounded our study site, ca. 150 km north of the modern limit of northern taiga, and T_{mija} was ca. 3°C higher than at present.
- The reconstructed Holocene temperature pattern in northeast European Russia near the Ural Mountains is markedly similar with that of the rest of northern Europe, with temperature reconstructions from Fennoscandia showing similar timing of the HTM at ca. 8000–4000 cal yr BP.
- There is a clear disparity between the early-Holocene peak in summer insolation and the mid-Holocene maximum of pollen-based reconstructed T_{mija} . This supports the possible role, as suggested by earlier modelling results, of albedo and meltwater forcing of the Laurentide ice sheet, mediated through the intensity of the North Atlantic thermohaline circulation, in delaying the HTM farfield in northeast European Russia.
- Late-Holocene cooling in the region started at ca. 3500 cal yr BP causing a rapid retreat of *Picea* treeline and triggering an abrupt initiation and activation of permafrost processes. Thus, the results suggest a major expansion of the northern Russian tundra during the last 3500 yr.

Acknowledgments

This study was financed by the CARBO-North project (EU Sixth Framework Programme, Global Change and Ecosystems subprogramme, project number 036993), the TUNDRA project (European Commission 4th Framework Funding 'Environment and Climate' Programme, Contract Nr. ENV4-CT97-0522), and Academy of Finland grants 47095 and 210879 (ARCTICA and HOT projects, respectively). Angela Self was funded by a NERC-CASE studentship. Samples were radiocarbon dated at the NERC-Radiocarbon Facility (Environment) and SUERC AMS Laboratory, East Kilbride, UK under allocation numbers 1243.1007 and 1289.0408. Charlotte Sweeney is thanked for help in identification of conifer stomata.

References

- Andreev, A.A., Klimanov, V.A., 2000. Quantitative Holocene climatic reconstruction from Arctic Russia. *Journal of Paleolimnology* 24, 81–91.
- Andreev, A.A., Manley, W.F., Ingólfsson, Ó., Forman, S.L., 2001. Environmental changes on Yukorski Peninsula, Kara Sea, Russia, during the last 12, 800 radiocarbon years. *Global and Planetary Change* 31, 255–264.
- Andreev, A.A., Siegert, C., Klimanov, V.A., Derevyagin, A.Y., Shilova, G.N., Melles, M., 2002. Last Pleistocene and Holocene vegetation and climate on the Taymyr lowland, northern Siberia. *Quaternary Research* 57, 138–150.
- Andreev, A.A., Tarasov, P.E., Ilyashuk, B.P., Ilyashuk, E.A., Cremer, H., Hermichen, W.-D., Wischer, F., Hubberten, H.-W., 2005. Holocene environmental history recorded in Lake Lyadhej-To sediments, Polar Urals, Russia. *Palaeogeography Palaeoclimatology Palaeoecology* 223, 181–203.
- ACIA (Arctic Climate Impact Assessment), 2004. Impacts of a Warming Arctic: Arctic Climate Impact Assessment. Cambridge University Press, Cambridge.
- Appleby, P.G., Oldfield, F., 1978. The calculation of ^{210}Pb dates assuming a constant rate of supply of unsupported ^{210}Pb to the sediment. *Catena* 5, 1–8.
- Berger, A., Loutre, M.F., 1991. Insolation values for the climate of the last 10 million of years. *Quaternary Science Reviews* 10, 297–317.
- Betts, R.A., 2000. Offset of the potential carbon sink from boreal forestation by decreases in surface albedo. *Nature* 408, 187–190.
- Bigelow, N.H., Brubaker, L.B., Edwards, M.E., Harrison, S.P., Prentice, I.C., Anderson, P.M., Andreev, A.A., Bartlein, P.J., Christensen, T.R., Cramer, W., Kaplan, J.O., Lozhkin, A.V.,

- Matveyeva, N.V., Murray, D.F., McGuire, A.D., Razzhivin, V.Y., Ritchie, J.C., Smith, B., Walker, D.A., Kremenetski, K., Paus, A., Pisaric, M.F.J., Volkova, V.S., 2003. Climate change and Arctic ecosystems: 1. Vegetation changes north of 55°N between the last glacial maximum, mid-Holocene, and present. *Journal of Geophysical Research* 108, 8170.
- Binney, H.A., Willis, K.J., Edwards, M.E., Bhagwat, S.A., Anderson, P.A., Andreev, A.A., Blaauw, M., Damblon, F., Haesaerts, P., Kienast, F., Kremenetski, K.V., Krivonogov, S.K., Lozhkin, A.V., MacDonald, G.M., Novenko, E.Y., Oksanen, P., Sapelko, T.V., Välranta, M., Vazhenina, L., 2009. The distribution of late-Quaternary woody taxa in northern Eurasia: evidence from a new macrofossil database. *Quaternary Science Reviews* 28, 2445–2464.
- Birks, H.J.B., Birks, H.J.B., 2003. Reconstructing Holocene Climates from Pollen and Plant Macrofossils. In: Mackay, A., Battarbee, R., Birks, J., Oldfield, F. (Eds.), *Global Change in the Holocene*. Arnold, London, pp. 342–357.
- Birks, H.J.B., Line, J.M., Juggins, S., Stevenson, A.C., ter Braak, C.J.F., 1990. Diatoms and pH reconstruction. *Philosophical Transactions of the Royal Society of London. Series B* 327, 263–278.
- Birks, H.J.B., 1986. Late-Quaternary biotic changes in terrestrial and lacustrine environments, with particular reference to north-west Europe. In: Berglund, B.E. (Ed.), *Handbook of Holocene Palaeoecology and Palaeohydrology*. Wiley, Chichester, pp. 3–66.
- Birks, H.J.B., 1998. Numerical tools in quantitative palaeolimnology—progress, potentialities, and problems. *Journal of Paleolimnology* 20, 301–332.
- Birks, H.J.B., 2003. Quantitative palaeoenvironmental reconstructions from Holocene biological data. In: Mackay, A., Battarbee, R., Birks, J., Oldfield, F. (Eds.), *Global Change in the Holocene*. Arnold, London, pp. 107–123.
- Birks, H.J.B., Seppä, H., 2004. Pollen-based reconstructions of late-Quaternary climate in Europe—progress, problems and pitfalls. *Acta Palaeobotanica* 44, 317–334.
- Bonan, G.B., 2008. Forests and climate change: forcings, feedbacks, and the climate benefits of forests. *Science* 320, 1444–1449.
- Bronk Ramsey, C., 1995. Radiocarbon calibration and analysis of stratigraphy: the OxCal program. *Radiocarbon* 37, 425–430.
- Bronk Ramsey, C., 2009. Bayesian analysis of radiocarbon dates. *Radiocarbon* 51, 337–360.
- Chapin III, F.S., Sturm, M., Serreze, M.C., McFadden, J.P., Key, J.R., Lloyd, A.H., McGuire, A.D., Rupp, T.S., Lynch, A.H., Schimel, J.P., Beringer, J., Chapman, W.L., Epstein, H.E., Euskirchen, E.S., Hinzman, L.D., Jia, G., Ping, C.-L., Tape, K.D., Thompson, C.D.C., Walker, D.A., Welker, J.M., 2005. Role of land-surface changes in arctic summer warming. *Science* 310, 657–660.
- Christensen, J.H., Hewitson, B., Busuioic, A., Chen, A., Gao, X., Held, I., Jones, R., Kolli, R.K., Kwon, W.-T., Laprise, R., Magaña Rueda, V., Mearns, L., Menéndez, C.G., Räisänen, J., Rinke, A., Sarr, A., Whetton, P., 2007. Regional Climate Projections. In: Solomon, S., Qin, D., Manning, M., Chen, Z., Marquis, M., Avery, K.B., Tignor, M., Miller, H.L. (Eds.), *Climate Change 2007: The Physical Science Basis. Contribution of Working Group I to the Fourth Assessment Report of the Intergovernmental Panel on Climate Change*. Cambridge University Press, Cambridge, pp. 847–940.
- Cremer, H., Andreev, A., Hubberten, H.-W., Wischer, F., 2004. Paleolimnological reconstructions of Holocene environments and climate from lake Lyadhej-To, Ural Mountains, Northern Russia. *Arctic, Antarctic, and Alpine Research* 36, 147–155.
- Davis, M.B., 1986. Climatic instability, time lags, and community disequilibrium. In: Diamond, J.M., Case, T.L. (Eds.), *Community Ecology*. Harper and Rowe, New York, pp. 269–284.
- deMenocal, P., Ortiz, J., Guilderson, T., Adkins, J., Sarnthein, M., Baker, L., Yarusinsky, M., 2000. Abrupt onset and termination of the African Humid Period: rapid climate responses to gradual insolation forcing. *Quaternary Science Reviews* 19, 347–361.
- Euskirchen, E.S., McGuire, A.D., Chapin III, F.S., Yi, S., Thompson, C.C., 2009. Changes in vegetation in northern Alaska under scenarios of climate change, 2003–2100: implications for climate feedbacks. *Ecological Applications* 19, 1022–1043.
- Fægri, K., Iversen, J., 1989. *Textbook of Pollen Analysis*. Wiley, Chichester.
- Fischlin, A., Midgley, G.F., Price, J.T., Leemans, R., Gopal, B., Turley, C., Rounsevell, M.D.A., Dube, O.P., Tarazona, J., Velichko, A.A., 2007. Ecosystems, their properties, goods, and services. In: Parry, M.L., Canziani, O.F., Palutikof, J.P., van der Linden, P.J., Hanson, C.E. (Eds.), *Climate Change 2007: Impacts. Adaptation and Vulnerability. Contribution of Working Group II to the Fourth Assessment Report of the Intergovernmental Panel on Climate Change*. Cambridge University Press, Cambridge, pp. 211–272.
- Foley, J.A., Kutzbach, J.E., Coe, M.T., Levis, S., 1994. Feedbacks between climate and boreal forests during the Holocene epoch. *Nature* 371, 52–54.
- Foley, J.A., Heil Costa, M., Delire, C., Ramankutty, N., Snyder, P., 2003. Green surprise? How terrestrial ecosystems could affect earth's climate. *Frontiers in Ecology and the Environment* 1, 38–44.
- Ganopolski, A., Kubatzki, C., Claussen, M., Brovkin, V., Petoukhov, V., 1998. The influence of vegetation-atmosphere-ocean interaction on climate during the mid-Holocene. *Science* 280, 1916–1919.
- Gorczyński, L., 1920. Sur le calcul du degré du continentalisme et son application dans la climatologie. *Geografiska Annaler* 2, 324–331.
- Gorczyński, L., 1922. The calculation of the degree of continentality. *Monthly Weather Reviews* 7, 370.
- Heegaard, E., Birks, H.J.B., Telford, R.J., 2005. Relationships between calibrated ages and depth in stratigraphical sequences: an estimation procedure by mixed-effect regression. *The Holocene* 15, 612–618.
- Hijmans, R.J., Cameron, S.E., Parra, J.L., Jones, P.G., Jarvis, A.J., 2005. Very high resolution interpolated climate surfaces for global land areas. *International Journal of Climatology* 25, 1965–1978.
- Hinzman, L.D., Bettez, N.D., Bolton, W.R., et al., 2005. Evidence and implications of recent climate change in northern Alaska and other arctic regions. *Climatic Change* 72, 251–298.
- Huntley, B., 1993. The use of climate response surfaces to reconstruct palaeoclimate from Quaternary pollen and plant macrofossil data. *Philosophical Transactions of the Royal Society, London B* 341, 215–224.
- Jones, V.J., Leng, M.J., Solovieva, N., Sloane, H.J., Tarasov, P., 2004. Holocene climate of the Kola Peninsula: evidence from the oxygen isotope record of diatom silica. *Quaternary Science Reviews* 23, 833–839.
- Jones, V.J., Solovieva, N., Self, A.E., McGowan, S., Rosén, P., Salonen, J.S., Seppä, H., Välranta, M., Parrott, E., Brooks, S.J., in press. The influence of Holocene tree-line advance and retreat on an arctic lake ecosystem; a multi-proxy study from Kharine Lake, North Eastern European Russia. *Journal of Paleolimnology*.
- Juggins, S., 2007. C2 Version 1.5 User guide. Software for ecological and palaeoecological data analysis and visualisation. Newcastle University, Newcastle upon Tyne.
- Kaakinen, A., Eronen, M., 2000. Holocene pollen stratigraphy indicating climatic and tree-line changes derived from a peat section at Ortino, in the Pechora lowland, northern Russia. *The Holocene* 10, 611–620.
- Kaplan, J.O., Bigelow, N.H., Prentice, I.C., Harrison, S.P., Bartlein, P.J., Christensen, T.R., Cramer, W., Matveyeva, N.V., McGuire, A.D., Murray, D.F., Razzhivin, V.Y., Smith, B., Walker, D.A., Anderson, P.M., Andreev, A.A., Brubaker, L.B., Edwards, M.E., Lozhkin, A.V., 2003. Climate change and Arctic ecosystems: 2. Modeling, paleodata-model comparisons, and future projections. *Journal of Geophysical Research* 108, 8171.
- Kaufman, D.S., Schneider, D.P., McKay, N.P., Ammann, C.M., Bradley, R.S., Briffa, K.R., Miller, G.H., Otto-Bliesner, P.L., Overpeck, J.T., Arctic Lakes 2k Project Members (Abbott, M., Axford, Y., Bird, B., Birks, H.J.B., Bjune, A.E., Briner, J., Cook, T., Chipman, M., Gajewski, K., Geirsdottir, A., Hu, F.S., Kutchko, B., Lamoureux, S., Loso, M., MacDonald, G.M., Peros, M., Porinchu, D., Schiff, C., Seppä, H., Thomas, E.), 2009. Recent warming reverses long-term arctic cooling. *Science* 325, 1236–1239.
- Khotinskiy, N.A., 1984. Holocene Vegetation History. In: Velichko, A.A. (Ed.), *Late Quaternary Environments of the Soviet Union*. Longman, London, pp. 179–200.
- Kremenetski, C.V., Sulerzhitsky, L.D., Hantemirov, R., 1998. Holocene history of the Northern Range limits of some trees and shrubs in Russia. *Arctic and Alpine Research* 30, 317–333.
- Kultti, S., Välranta, M., Sarmaja-Korjonen, K., Solovieva, N., Virtanen, T., Kauppi, T., Eronen, M., 2003. Palaeoecological evidence of changes in vegetation and climate during the Holocene in the pre-Polar Urals, northeast European Russia. *Journal of Quaternary Science* 18, 503–520.
- Kultti, S., Oksanen, P., Välranta, M., 2004. Holocene tree line, permafrost, and climate dynamics in the Nenets Region, East European Arctic. *Canadian Journal of Earth Sciences* 41, 1141–1158.
- MacDonald, G.M., Velichko, A.A., Kremenetski, C.V., Borisova, O.K., Goleva, A.A., Andreev, A.A., Cwynar, L.C., Riding, R.T., Forman, S.L., Edwards, T.W.D., Aravena, R., Hammarlund, D., Szeicz, J.M., Gattaulin, V.N., 2000. Holocene treeline history and climate change across northern Eurasia. *Quaternary Research* 53, 302–311.
- MacDonald, G.M., Kremenetski, K.V., Beilman, D.W., 2008. Climate change and the northern Russian treeline zone. *Philosophical Transactions of the Royal Society of London. Series B* 363, 2285–2299.
- MacDonald, G.M., 2010. Some Holocene palaeoclimatic and palaeoenvironmental perspectives on Arctic/Subarctic climate warming and the IPCC 4th Assessment Report. *Journal of Quaternary Science* 25, 39–47.
- Mangerud, J., Svendsen, J.I., Astakhov, V.I., 1999. Age and extent of the Barents and Kara ice sheets in Northern Russia. *Boreas* 28, 46–80.
- Mangerud, J., Jakobsson, M., Alexanderson, H., Astakhov, V., Clarke, G.K.C., Henriksen, M., Hjort, C., Krinner, G., Lunkka, J.-P., Möller, P., Murray, A., Nikolskaya, O., Saarnisto, M., Svendsen, J.I., 2004. Ice-dammed lakes and rerouting of the drainage of northern Eurasia during the Last Glaciation. *Quaternary Science Reviews* 23, 1313–1332.
- Mazhitova, G., Oberman, N., 2003. Permafrost of the Usa River Basin. Digital Media. National Snow and Ice Data Center/World Data Center for Glaciology, Boulder, Colorado. http://nsidc.org/data/docs/gfcd/ggd614_map_usariver/ (12 March 2009).
- Meehl, G.A., Stocker, T.F., Collins, W.D., Friedlingstein, P., Gaye, A.T., Gregory, J.M., Kitoh, A., Knutti, R., Murphy, J.M., Noda, A., Raper, S.C.B., Watterson, I.G., Weaver, A.J., Zhao, Z.-C., 2007. Global climate projections. In: Solomon, S., Qin, D., Manning, M., Chen, Z., Marquis, M., Avery, K.B., Tignor, M., Miller, H.L. (Eds.), *Climate Change 2007: The Physical Science Basis. Contribution of Working Group I to the Fourth Assessment Report of the Intergovernmental Panel on Climate Change*. Cambridge University Press, Cambridge, pp. 747–845.
- Miller, G.H., Alley, R.B., Brigham-Grette, J., Fitzpatrick, J.J., Polyak, L., Serreze, M.C., White, J.W.C., 2010a. Arctic amplification: can the past constrain the future? *Quaternary Science Reviews* 29, 1779–1790.
- Miller, G.H., Brigham-Grette, J., Alley, R.B., Anderson, L., Bauch, H.A., Douglas, M.S.V., Edwards, M.E., Elias, S.A., Finney, B.P., Fitzpatrick, J.J., Funder, S.V., Herbert, T.D., Hinzman, L.D., Kaufman, D.S., MacDonald, G.M., Polyak, L., Robock, A., Serreze, M.C., Smol, J.P., Spielhagen, R., White, J.W.C., Wolfe, A.P., Wolff, E.W., 2010b. Temperature and precipitation history of the Arctic. *Quaternary Science Reviews* 29, 1679–1715.
- Moore, P.D., Webb, J.A., Collinson, M.E., 1991. *Pollen Analysis*. Blackwell, Oxford.
- Oksanen, P.O., Kuhry, P., Alekseeva, R.N., 2001. Holocene development of the Rogovaya River peat plateau, European Russian Arctic. *The Holocene* 11, 25–40.
- Oksanen, P.O., 2005. Development of palsa mires on the northern European continent in relation to Holocene climatic and environmental changes. PhD thesis. *Acta Universitatis Ouluensis A* 446.
- Paus, A., Svendsen, J.I., Matiouchkov, A., 2003. Late Weichselian (Valdaian) and Holocene vegetation and environmental history of the northern Timan Ridge, European Arctic Russia. *Quaternary Science Reviews* 22, 2285–2302.
- Payette, S., Eronen, M., Jasinski, P., 2002. The circumboreal tundra-trait interface: late Pleistocene and Holocene changes. *Ambio Special Report* 12, 15–22.

- Prentice, I.C., 1980. Multidimensional scaling as a research tool in Quaternary palynology: a review of theory and methods. *Review of Palaeobotany and Palynology* 31, 71–104.
- R Development Core Team, 2008. R: A language and environment for statistical computing. R Foundation for Statistical Computing, Vienna, Austria. <http://www.R-project.org>.
- Reimer, P.J., Baillie, M.G.L., Bard, E., Bayliss, A., Beck, J.W., Blackwell, P.G., Bronk Ramsey, C., Buck, C.E., Burr, G.S., Edwards, R.L., Friedrich, M., Grootes, P.M., Guilderson, T.P., Hajdas, I., Heaton, T.J., Hogg, A.G., Hughen, K.A., Kaiser, K.F., Kromer, B., McCormac, F.G., Manning, S.W., Reimer, R.W., Richards, D.A., Southon, J.R., Talamo, S., Turney, C.S.M., van der Plicht, J., Weyhenmeyer, C.E., 2009. IntCal09 and Marine09 radiocarbon age calibration curves, 0–50, 000 years cal BP. *Radiocarbon* 51, 1111–1150.
- Rekacewicz, P., 1998. Ecosystems of Northwest Russia. Barentswatch Atlas, GRID-Arendal, United Nations Environment Programme. http://maps.grida.no/go/graphic/ecosystems_in_northwest_russia (3 April 2009).
- Renssen, H., Seppä, H., Heiri, O., Roche, D.M., Goosse, H., Fichefet, T., 2009. The spatial and temporal complexity of the Holocene thermal maximum. *Nature Geoscience* 2, 411–414.
- Ritchie, J.C., 1986. Climate change and vegetation response. *Vegetatio* 67, 65–74.
- Sarmaja-Korjonen, K., Kultti, S., Solovieva, N., Välranta, M., 2003. Mid-Holocene palaeoclimatic and palaeohydrological conditions in northeastern European Russia: a multi-proxy study of Lake Vankavä. *Journal of Paleolimnology* 30, 415–426.
- Seppä, H., Birks, H.J.B., 2001. July mean temperature and annual precipitation trends during the Holocene in the Fennoscandian tree-line area: pollen-based climate reconstructions. *Holocene* 11, 527–537.
- Seppä, H., Nyman, M., Korhola, A., Weckström, J., 2002. Changes of tree-lines and alpine vegetation in relation to post-glacial climate changes in northern Fennoscandia based on pollen and chironomid records. *Journal of Quaternary Science* 17, 287–301.
- Seppä, H., Birks, H.J.B., Odland, A., Poska, A., Veski, S., 2004. A modern pollen–climate calibration set from northern Europe: developing and testing a tool for palaeoclimatological reconstructions. *Journal of Biogeography* 31, 251–267.
- Seppä, H., Hammarlund, D., Antonsson, K., 2005. Low-frequency and high-frequency changes in temperature and effective humidity during the Holocene in southcentral Sweden: implications for atmospheric and oceanic forcings of climate. *Climate Dynamics* 25, 285–297.
- Seppä, H., MacDonald, G.M., Birks, H.J.B., Gervais, B.R., Snyder, J.A., 2008. Late-Quaternary summer temperature changes in the North-European tree-line region. *Quaternary Research* 69, 404–412.
- Seppä, H., Björne, A.E., Telford, R.J., Birks, H.J.B., Veski, S., 2009. Last nine-thousand years of temperature variability in Northern Europe. *Climate Past* 5, 523–535.
- Serebryanny, L., Andreev, A., Malyasova, E., Tarasov, P., Romanenko, F., 1998. Lateglacial and early-Holocene environments of Novaya Zemlya and the Kara Sea Region of the Russian Arctic. *Holocene* 8, 323–330.
- Snyder, J.A., MacDonald, G.M., Forman, S.L., Tarasov, G.A., Mode, W.N., 2000. Postglacial climate and vegetation history, north-central Kola Peninsula, Russia: pollen and diatom records from Lake Yarnyshnoe-3. *Boreas* 26, 329–346.
- Steig, E.J., 1999. Mid Holocene climate change. *Science* 286, 1485–1487.
- Stockmarr, J., 1971. Tablets with spores used in absolute pollen analysis. *Pollen Spores* 13, 615–621.
- Svensen, J.I., Astakhov, V.I., Yu, D., Bolshiyakov, I.D., Dowdeswell, J.A., Gataullin, V., Hjort, C., Hubberten, H.W., Larsen, E., Mangerud, J., Melles, M., Möller, P., Saarnisto, M., Siebert, M.J., 1999. Maximum extent of the Eurasian ice sheets in the Barents and Kara Sea region during the Weichselian. *Boreas* 28, 234–242.
- Svensen, J.I., Alexanderson, H., Astakhov, V.I., Demidov, I., Dowdeswell, J.A., Funder, S., Gataullin, V., Henriksen, M., Hjort, C., Houmark-Nielsen, M., Hubberten, H.W., Ingólfsson, Ó., Jakobsson, M., Kjær, K.H., Larsen, E., Lokrantz, H., Lunkka, J.P., Lyså, A., Mangerud, J., Matoriouchkov, A., Murray, A., Möller, P., Niessen, F., Nikolskaya, O., Polyak, L., Saarnisto, M., Siebert, C., Siefert, M.J., Spielhagen, R.F., Stein, R., 2004. Late Quaternary ice sheet history of northern Eurasia. *Quaternary Science Reviews* 23, 1229–1271.
- Swann, A.L., Fung, I.Y., Levis, S., Bonan, G.B., Doney, S.C., 2010. Changes in Arctic vegetation amplify high-latitude warming through the greenhouse effect. *Proceedings of the National Academy of Science* 107, 1295–1300.
- Sweeney, C.A., 2004. A key for identification of stomata of the native conifers of Scandinavia. *Review of Palaeobotany and Palynology* 128, 281–290.
- Tarasov, P.E., Webb III, T., Andreev, A.A., Afanas'eva, N.B., Berezina, N.A., Bezusko, L.G., Blyakharchuk, T.A., Bolikhovskaya, N.S., Cheddadi, R., Chernavskaya, M.M., Chernova, G.M., Dorofeyuk, N.I., Dirksen, V.G., Elina, G.A., Filimonova, L.V., Glebov, F.Z., Guiot, J., Gunova, V.S., Harrison, S.P., Jolly, D., Khomutova, V.I., Kvavadze, E.V., Osipova, I.M., Panova, N.K., Prentice, I.C., Saarse, L., Sevastyanov, D.V., Volkova, V.S., Zernitskaya, V.P., 1998. Present-day and mid-Holocene biomes reconstructed from pollen and plant macrofossil data from the former Soviet Union and Mongolia. *Journal of Biogeography* 25, 1029–1053.
- Taskaev, A.I., Gladkov, V.P., Degtereva, S.V., Alekseeva, R.N., 1996. Okhranyaemye prirodnye territorii Respubliki Komi ("Protected natural areas of the Komi Republic", in Russian). Map. Scale 1:200, 000. Edited by G.V. Kvorov. VTU Gsh, Saint Petersburg.
- ter Braak, C.J.F., Juggins, S., 1993. Weighted averaging partial least squares regression (WA-PLS): an improved method for reconstructing environmental variables from species assemblages. *Hydrobiologia* 269 (270), 485–502.
- Tinner, W., Bigler, C., Gedy, S., Gregory-Eaves, I., Jones, R.T., Kaltenrieder, P., Krähenbühl, U., Hu, F.-S., 2008. A 700-year palaeoecological record of boreal ecosystem responses to climatic variation from Alaska. *Ecology* 89, 729–743.
- Välranta, M., Kaakinen, A., Kuhry, P., 2003. Holocene climate and landscape evolution East of the Pechora Delta, East-European Russian Arctic. *Quaternary Research* 59, 335–344.
- Välranta, M., Kultti, S., Seppä, H., 2006. Vegetation dynamics during the Younger Dryas–Holocene transition in the extreme northern taiga zone, northeastern European Russia. *Boreas* 35, 202–212.
- Välranta, M., Kaakinen, A., Kuhry, P., Kultti, S., Salonen, J.S., Seppä, H., 2011. Scattered late-glacial and early-Holocene tree populations as dispersal nuclei for forest development in NE European Russia. *Journal of Biogeography* 38, 922–932.
- Velichko, A.A., Andreev, A.A., Klimanov, V.A., 1997. Climate and vegetation dynamics in the tundra and forest zone during the late glacial and Holocene. *Quaternary International* 41 (42), 71–96.
- Velichko, A.A., Catto, N., Drenova, A.N., Klimanov, V.A., Kremenetski, K.V., Nechaev, V.P., 2002. Climate changes in East Europe and Siberia at the Late glacial–Holocene transition. *Quaternary International* 91, 75–99.
- Virtanen, T., Mikkola, K., Nikula, A., Christensen, J.H., Mazhitova, G.G., Oberman, N.G., Kuhry, P., 2004. Modeling the location of the forest line in northeast European Russia with remotely sensed vegetation and GIS-based climate and terrain data. *Arctic, Antarctic, and Alpine Research* 36, 314–322.
- Wanner, H., Beer, J., Butikofer, J., Crowley, T.J., Cubasch, U., Flückiger, J., Goosse, H., Grosjean, M., Joos, F., Kaplan, J.O., Kuttel, M., Müller, S.A., Prentice, I.C., Solomina, O., Stocker, T.F., Tarasov, P., Wagner, M., Widmann, M., 2008. Mid- to Late Holocene climate change: an overview. *Quaternary Science Reviews* 27, 1791–1828.
- Winton, M., 2006. Amplified Arctic climate change: what does surface albedo feedback have to do with it? *Geophysical Research Letters* 33, L03701.
- Wohlfarth, B., Filimonova, L., Bennike, O., Björkman, L., Brunnberg, L., Lavrova, N., Demidov, I., Possnert, G., 2002. Late-glacial and early Holocene environmental and climatic change at lake Tambichozero, southeastern Russian Karelia. *Quaternary Research* 58, 261–272.